ELSEVIER

Biochimica et Biophysica Acta 1467 (2000) 27–38

BIOCHIMICA ET BIOPHYSICA ACTA
BBA

www.elsevier.com/locate/bba

Electrochemical and NMR spectroscopic investigations of the influence of the probe molecule Eu(fod)$_3$ on the permeability of lipid membranes to ions

K.D. Schulze [a,*], H. Sprinz [b]

[a] *Institute of Physical and Theoretical Chemistry, University of Leipzig, Linnéstr. 2, D-04103 Leipzig, Germany*
[b] *Research Unit 'Time-Resolved Spectroscopy', Faculty of Chemistry and Mineralogy, University of Leipzig, Permoserstr. 15, D-04318 Leipzig, Germany*

Received 17 November 1999; received in revised form 29 February 2000; accepted 14 March 2000

Abstract

Investigating the action of the fluorinated europium complex Eu(fod)$_3$ on lipid membranes we found that the complex facilitates the ion transfer through the membrane. Electric measurements on planar lipid membranes showed that the membrane conductivity increases considerably by insertion of the complex into the membrane. The increase in the conductivity was only obtained if both layers of the membrane were modified with the complex. ^{1}H NMR spectroscopic studies using DOPC liposomes gave information about the location of the modifier complex in the lipid membrane. From chemical shift effects we concluded that the complex resides in the choline head group region of the membrane and also in the membrane interior near the –C=C– lipid double bond, but not in the center of the bilayer. For understanding of the mentioned conductivity effect we assume that the europium complex induces defects of yet unknown structure in the lipid matrix which provide paths for the ion transfer through the membrane. As appropriate measurements revealed, these paths seem to conduct cations predominantly. Investigating the current–voltage behavior of the modified lipid membranes in dependence on the ion concentration we obtained different shaped current–voltage curves. Calculation showed that a model with only one energy barrier inside the membrane is unable to describe these curves kinetically. However, by assuming two energy barriers – one barrier in each membrane lipid layer – the observed curve can be described satisfactorily.

Keywords: Lipid membrane; Ion permeability; Europium; ^{1}H nuclear magnetic resonance spectroscopy; Current–voltage curve; Impedance spectroscopy

1. Introduction

The lanthanide complex tris-6,6,7,7,8,8,8-heptafluor-2,2-dimethyl-3,5-octanedionato-europium (Eu(fod)$_3$) is widely used as a probe molecule for different spectroscopic investigations. Because of the complexing properties of the europium atom, the molecule strongly interacts with nucleophile molecule residues, e.g. with hydroxyl or amino groups. The presence of the paramagnetic europium changes the magnetic properties in the molecule under study connected to a shift and an expansion of the nuclear magnetic resonance (NMR) signals. Frequently, the mentioned shift effect enables a better separation of

* Corresponding author. Fax: +49-341-9736399;
E-mail: kdschulz@sonne.tachemie.uni-leipzig.de

0005-2736/00/$ – see front matter
PII: S0005-2736(00)00193-0

the NMR signals [1]. Besides in NMR spectroscopy $Eu(fod)_3$ is applied as a probe molecule in luminescence techniques [2,3].

$Eu(fod)_3$ can be used not only for the investigation of single molecules in solution, but also for the study of ordered structures like biological membranes which consist of structurally and electrically different parts, namely the polar surfaces and the non-polar inner part of the membrane.

A question which has to be answered in connection with a possible use of $Eu(fod)_3$ for biomembrane investigations is that of the binding sites of the probe molecule which could be located either at the membrane surfaces or more in the membrane interior. This problem is connected with the nature of interactions between $Eu(fod)_3$ and the membrane lipid molecules. Another question we were interested in was that of the $Eu(fod)_3$ influence on the macroscopic properties of the membranes, like electric conductivity or mechanical stability. As a probe molecule $Eu(fod)_3$ should have no significant influence on the mentioned properties. The mentioned items concerning the influence of the europium complex on biomembranes are still not investigated as far as we know.

For studying the interaction of $Eu(fod)_3$ with biomembranes we used ^1H NMR spectroscopy coupled with a liposome techniques. The use of small liposomes makes it possible to detect a binding effect to organic ions on different chemical groups of the phospholipid membrane as demonstrated for the large hydrophobic anion tetraphenylborate in a previous paper [4]. The electric behavior in the presence of $Eu(fod)_3$ was studied at single lipid bilayer membranes by measuring the membrane current–voltage curves and by impedance spectroscopy. Impedance spectroscopy was recently used to estimate rate constants [5] and energy barriers [6] of the transfer of tetraphenylborate ions through lipid membranes of different chemical composition.

2. Materials and methods

Most of the investigations mentioned above were carried out with dioleoyl phosphatidylcholine (DOPC) membranes, consisting of a phosphocholine head group and of oleoyl hydrocarbon chains which have a double bond between the ninth and the tenth carbon atom of the chain. For one experiment we used another phospholipid, namely diphytanoyl phosphatidylcholine (DPhyPC), without any double bond in the phytanoyl hydrocarbon chain. The chemical structures of DPhyPC and the lanthanide complexes used for the study are depicted in Fig. 1.

The lanthanide complexes differ in the fluorine residues which are only present in the $Eu(fod)_3$ molecule. For the assignment of the shifted signals we also used $Pr(fod)_3$ in NMR studies.

The electrochemical investigations were carried out with planar lipid membranes (about 1 mm^2 area) using a standard technique which was described in [5]. The $Eu(fod)_3$ and $Eu(dpm)_3$ concentrations in the cell chambers were altered by the addition of equal amounts of a stock solution to the electrolyte. The adjustment of a new stationary state after the addition of the lanthanide complexes was controlled by measuring the impedance of the membrane. Usually, stationary conditions were reached 20–30 min after adding the europium complexes. The electrochemical measurements were performed with the Impedance System IM6 from Zahner Electric Corp. (Kronach, Germany).

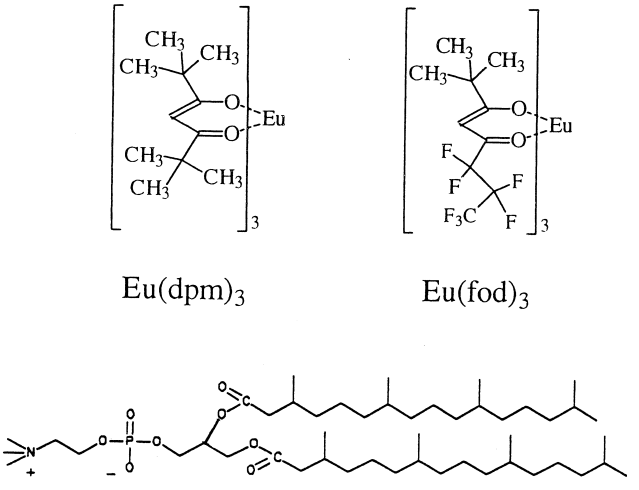

Fig. 1. Chemical structure of the used lanthanide complexes. $Eu(fod)_3$ = tris-6,6,7,7,8,8,8-heptafluor-2,2-dimethyl-3,5-octanedionato-europium. $Eu(dpm)_3$ = tris-2,2,6,6-tetramethyl-3,5-heptanedionato-europium (both substances were received from Fluka, Germany).

Liposomes of DOPC (Sigma, Deisenhofen, Germany) were produced by the procedure described in our previous paper [4]. The chloroform of the DOPC solution was removed in a rotary evaporator at 40°C and the remaining lipid film was exposed to high vacuum overnight. The phospholipid (12.7 mM) was then dispersed by addition of heavy water (Deuchem, Leipzig, Germany) at 99.8% D (0.1 M NaCl, pD 5.5), followed by shaking. Small unilamellar vesicles (SUV) were prepared by sonication (Sonopuls HD200, Bandelin, Berlin, Germany) above the phase transition under a stream of argon at 5°C. The obtained solution was centrifuged in order to remove titanium particles. The resulting bilayer vesicles have a diameter of about 30 nm (see [7]).

The incubation of liposomes with the shift reagent was performed using two methods: first, by adding a small amount of a solution of the shift reagent (15 mg/ml) in acetone-d6 (Deuchem, 99.8% D) to the liposomes, and second, by the following procedure: a solution of the shift reagent in chloroform was dried at 313 K on a rotary evaporator and then evacuated for 3 h in a high vacuum. The liposomal solution (3 ml) was added, and the vessel was shaken for 30 min at room temperature.

The micellar solution was prepared using hexadecyltrimethylammonium chloride (HTAC) from Aldrich (Deisenhofen, Germany).

^{1}H NMR experiments were performed at 295 K on a Bruker Avance DPX 250 spectrometer at the Institute of Surface Modification, Leipzig, Germany. Thirty-two scans were accumulated, using 32 000 data points. A 0.8 Hz exponential filter was used before Fourier transformation. Chemical shifts were determined using DSS as an internal standard. Overlapping signals were analyzed by the computer program PEAKFIT.

3. Experimental results

3.1. NMR results

Preliminary NMR experiments have shown that the effects of the shift reagents on the chemical shifts of the phospholipid molecule are independent of the mode of incubation of the paramagnetic complex with the lipid suspension (see Section 2). To characterize the hydrophobic properties of the complexes, we determined the partition coefficient between octanol and water, measuring the optical absorption in both phases after mixing and centrifugation. Even at high concentrations of the complex in the mixture (0.1 mM) it does not show any absorption in the UV-Vis region in the water phase. Therefore, both europium complexes were characterized by an octanol/water partition coefficient higher than 500:1. The comparison of the optical absorption of both europium complexes (0.1 mM) in methanolic solution and in HTAC micelles (80 mM) enables the detection of differences in the solubility in hydrocarbons. After incorporation into the micelles the enhancement of optical density in the case of the Eu(dpm)$_3$ spectrum was 20% more than that of Eu(fod)$_3$. This behavior [8] is an indication of the influence of fluorine groups that means an accumulation of the fluor-free complex Eu(dpm)$_3$ within the hydrophobic core of the micelles.

The interaction of Eu(fod)$_3$ with the fatty acid residues does not dramatically influence the structure of the liposome, otherwise one would expect line broadening effects in the NMR spectra. The line widths of all signals are not noticeably influenced up to a concentration of 1.5 mM Eu(fod)$_3$. However, above a concentration of 2 mM a broadening of the signals was observed, indicating a destruction of the bilayer. This finding is in accordance with observations on planar bilayer membranes used for the electric measurements. The line width of the water signal (0.8 Hz), measured at 1 h after mixing, shows line broadening effects, namely 1.4 Hz for DOPC without shift reagent, 2.7 Hz with 1.5 mM of Eu(fod)$_3$, and 5.0 Hz in the presence of 1.5 mM of Eu(dpm)$_3$. From this result one may expect that at least one binding site for the paramagnetic complexes is located at the vesicle surface leading to magnetic interactions with the lipid surface groups and with water from the hydration shell. In fact, the europium complexes induced upfield shifts for the proton signals of the fatty acid chains as well as downfield shifts for the choline residue. Additionally, we also determined the Pr(fod)$_3$-induced shifts on the lipid signals (Fig. 2).

However, these signal shifts were not uniform for the considered chemical groups, but showed a splitting into two components. This is demonstrated in

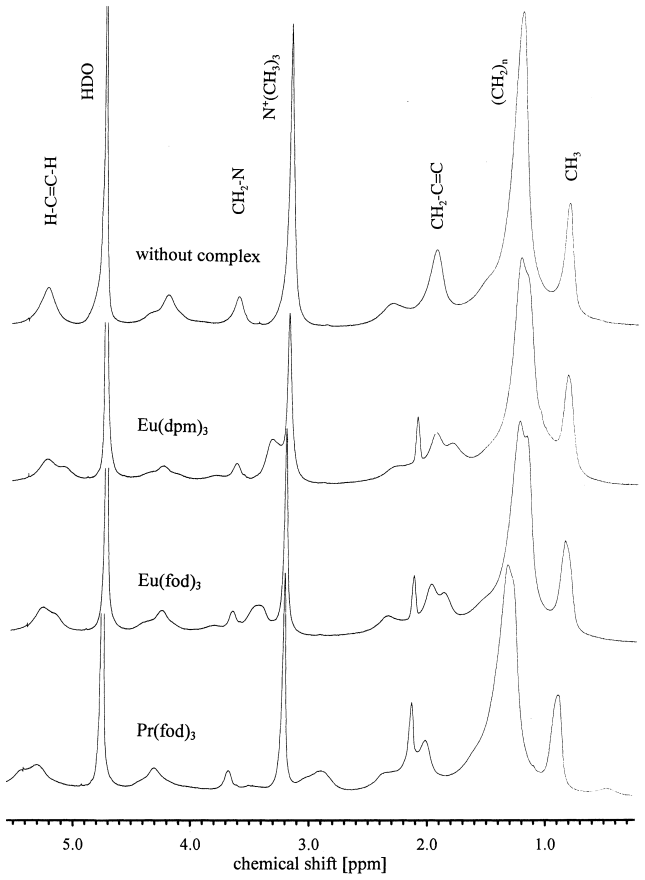

Fig. 2. ^{1}H NMR spectra of DOPC (12.7 mM in D_2O, 0.1 M NaCl) in the presence of various lanthanide complexes (1.5 mM). The signal at 2.1 ppm refers to acetone-d_5.

Fig. 3 for the methylene protons in α-position to the olefinic group.

With the aim of interpreting this unexpected split-

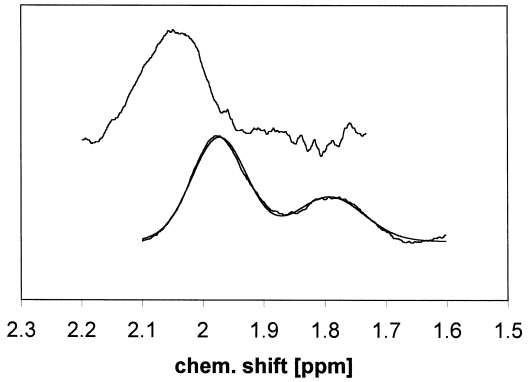

Fig. 3. ^{1}H NMR spectrum of the methylene protons in α-position to the olefinic group of DOPC liposomes. Top: without $Eu(fod)_3$; four scans below: with 2 mM $Eu(fod)_3$, spectrum recorded 1 h after mixing.

Table 1
Ratios of the areas of the split NMR signals for a hydrophilic and a hydrophobic group of DOPC (12.7 mM) in the presence of lanthanide complexes (n.d.: not determined)

Complex structure	$[(N(CH_3)_3^+]^a$	$[-C=C-]^b$
$Eu(fod)_3$	0.59 ± 0.05	0.54 ± 0.04
$Eu(dpm)_3$	0.58 ± 0.05	n.d.
$Pr(fod)_3$	0.49 ± 0.05	n.d.
Model (see [7])	0.49	0.49

[a]1.5 mM complex (see Fig. 2).
[b]2 mM complex (see Fig. 3).

ting behavior we performed a curve fitting procedure with a Gauss line shape using two curves characterized by half widths of 0.11 ppm and 0.13 ppm, respectively. The results of simulation of both bands are presented in Fig. 3.

Table 1 summarizes the calculations of the fraction of the areas of the strongly shifted signal component in relation to the weakly shifted signal component for two chemical groups of the liposome.

It is obvious from Table 1 that the fractions of the areas correspond very well to fractions of phospholipid molecules in the inner and the outer lipid layer, valid for our conditions of liposome preparation by ultrasound [7]. Therefore, the heterogeneous shifts can be explained by an asymmetric distribution of the shift reagent in the bilayer, namely, by an accumulation of the additive within the inner lipid layer. From the chemical shifts in Fig. 3 it can be estimated that the molar ratio [shift reagent]/[lipid molecule] within the inner lipid layer is more than three times higher in comparison to that ratio for the outer lipid layer.

Fig. 4 presents a compilation of lanthanide-in-

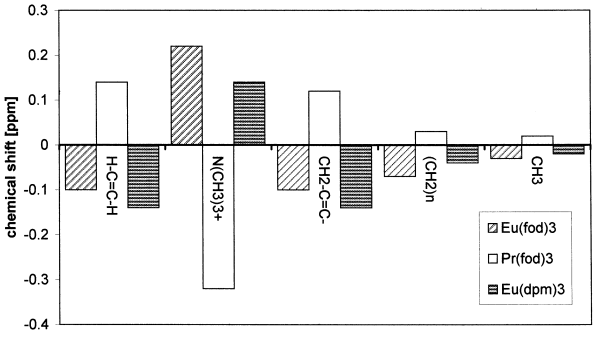

Fig. 4. Chemical shift effects of lanthanides (1.5 mM) on the ^{1}H NMR signals of DOPC (12.7 mM).

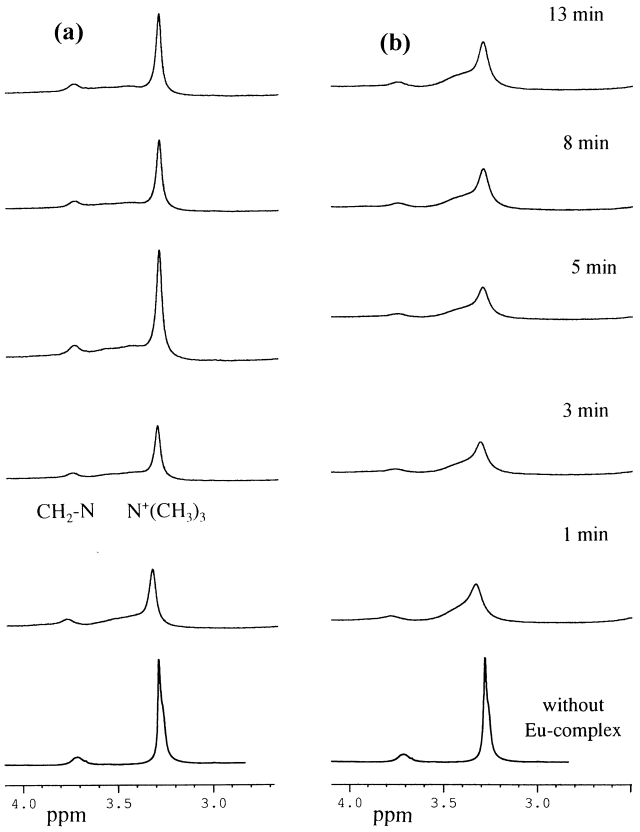

Fig. 5. Incubation experiments of DOPC (12.7 mM) liposomes (SUV) with the shift reagents (2 mM). ^{1}H NMR spectra of the choline head group were recorded at various times after mixing. a: $Eu(fod)_3$; b: $Eu(dpm)_3$.

duced chemical shifts on the various chemical groups of the phospholipid (using in each case the component with the maximum shift, which can be interpreted as the shift effect on the inner lipid layer where most of the complex should be located).

For the europium complexes upfield shifts were observed for all signals of the fatty acid residues, whereas one fraction of the choline signals showed large downfield shifts. According to Fig. 4, all the $Pr(fod)_3$-induced shifts show the expected opposite sign.

However, at the methyl groups of the fatty acid chains just small shift effects were detectable. This fact excludes an accumulation of the complex within the center region between the two lipid layers.

The comparison of the NMR spectra of the choline head group at different times after the addition of the europium complex demonstrates the time course of distribution of the shift reagent liposomes (Fig. 5).

Immediately after the addition, the shift reagent becomes bound to the membrane surface, characterized by line broadening and a downfield shift. Due to the higher concentration of the $Eu(fod)_3$ (in comparison to the experiments described in Fig. 4) the shifted component of the $N(CH)_3^+$ signal was broadened beyond the detection limit. The remaining signal of the $N(CH)_3^+$ protons becomes more narrow 3 min after mixing and the splitting of the hydrophobic signals reaches its maximum (shown in Fig. 3). In the presence of $Eu(dpm)_3$ the choline signal remains broad even at 13 min after mixing, but in contrast to $Eu(fod)_3$ the second signal component was detectable as a broad shoulder.

3.2. Electrochemical investigations

For studying the influence of $Eu(fod)_3$ on the membrane conductivity, we carried out different measurements in sodium chloride solutions. At first, we varied the $Eu(fod)_3$ concentration. Fig. 6 gives the appropriate impedance spectra.

The right parts of the spectra are governed by the membrane capacitance as can be seen by the −45° decay of the impedance at high frequencies whereas the left part of the spectra is determined by the ohmic membrane resistance.

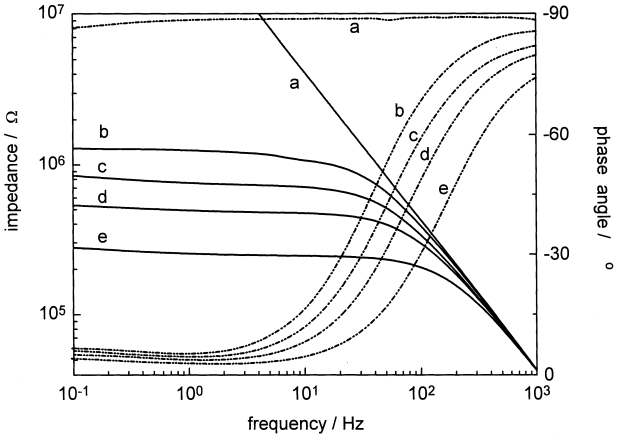

Fig. 6. Influence of $Eu(fod)_3$ on the impedance spectrum and on the phase angle of a DOPC lipid membrane. $Eu(fod)_3$ concentrations (in μM): a = 0, b = 10, c = 20, d = 30, e = 50; solid line = impedance; dashed line = phase angle, electrolyte: 0.1 M NaCl; membrane area: 1.5 mm^2.

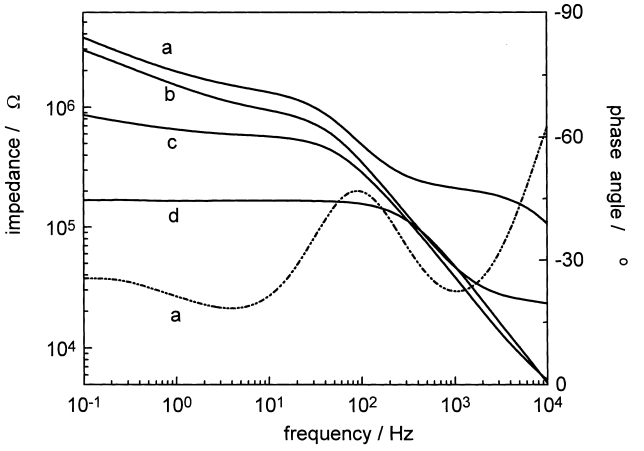

Fig. 7. Influence of various NaCl concentrations on the impedance spectrum and on the phase angle of a $Eu(fod)_3$-modified DOPC membrane. NaCl concentrations (in M): a = 0.001, b = 0.01, c = 0.1, d = 1; solid line = impedance; dashed line = phase angle; $Eu(fod)_3$ concentration: 50 μM; membrane area: 1.1 mm^2.

In the case where no modifier is added (Fig. 6a), the impedance spectrum is governed by the membrane capacitance over the whole depicted frequency range. Fig. 6 shows that the ion transfer resistance decreases with increasing $Eu(fod)_3$ concentration whereas the membrane capacitance obviously does not change.

For the experiments described above $Eu(fod)_3$ was given to both sides of the membrane. We also studied the electric membrane behavior when $Eu(fod)_3$ was added only to one membrane side. In this case, we frequently found no reduction of the membrane impedance. Only when $Eu(fod)_3$ was added to the other side, a decrease of the low frequency impedance was observed.

It should be mentioned at least that for large $Eu(fod)_3$ concentrations (>100 μM) the mechanical stability of the bilayer membrane in the Teflon hole vanishes and the former planar membrane changes to a more hemispheric one which slowly increases in its diameter up to the destruction of the membrane.

In the following experiments, we varied the sodium chloride concentration while the $Eu(fod)_3$ concentration was held constant. The electrolyte concentration was varied over three orders of magnitude.

Increasing the NaCl concentration decreases the membrane resistance as illustrated in Fig. 7. The resistance does not decrease to the same extent as the concentration increases. Possible explanations for this will be given in Section 5.

Fig. 7 also shows that the impedance at low frequencies increases considerably. This increase and the frequency course of the phase angle (Fig. 6a, dashed line) which approximates to −30° indicate a diffusion influence on the impedance spectra. As expected, this influence is most distinct for the lower NaCl concentrations.

In the impedance spectra Fig. 7a,b, a second ohmic component at higher frequencies occurs. This component refers to the ohmic resistance of the NaCl solution which increases with the decrease of the electrolyte concentration.

In addition to the impedance spectra in Fig. 7, we also registered the current–voltage curves of the membrane (Fig. 8A–D).

The curves were measured under potentiodynamic conditions. A variation of the scan rate in the range of 0.5–5 mV/s changed neither the current nor the hysteresis of the curves significantly. Most of the curves have an exponential shape (Fig. 8B–D), but sometimes we also measured curves with a distinctly different current course as illustrated in Fig. 8E,F.

The curve in Fig. 8E which has only a slight nonlinear course was also registered in 0.1 M NaCl solution as the curve in Fig. 8C with its exponential shape. This difference illustrates that the shape of curves can vary from membrane to membrane.

Generally, the measured current–voltage curves have roughly the same course in both current directions (symmetrical curve behavior).

The described experimental findings concerning the shape of the membrane current–voltage curves assisted us in choosing a suitable physico-chemical model for the description of the $Eu(fod)_3$-facilitated ion transfer (see Section 4).

The experiments described above revealed a strong influence of $Eu(fod)_3$ on the membrane conductivity. $Eu(fod)_3$ obviously enhances the ion transfer through the lipid membrane. In this connection, the question arose of what kind of ion(s) are enabled to permeate by $Eu(fod)_3$.

To answer this question we carried out measurements of the membrane potential resulting from NaCl gradients across the membrane. In the experiments, the concentration in one chamber was held constant while the concentration in the other cham-

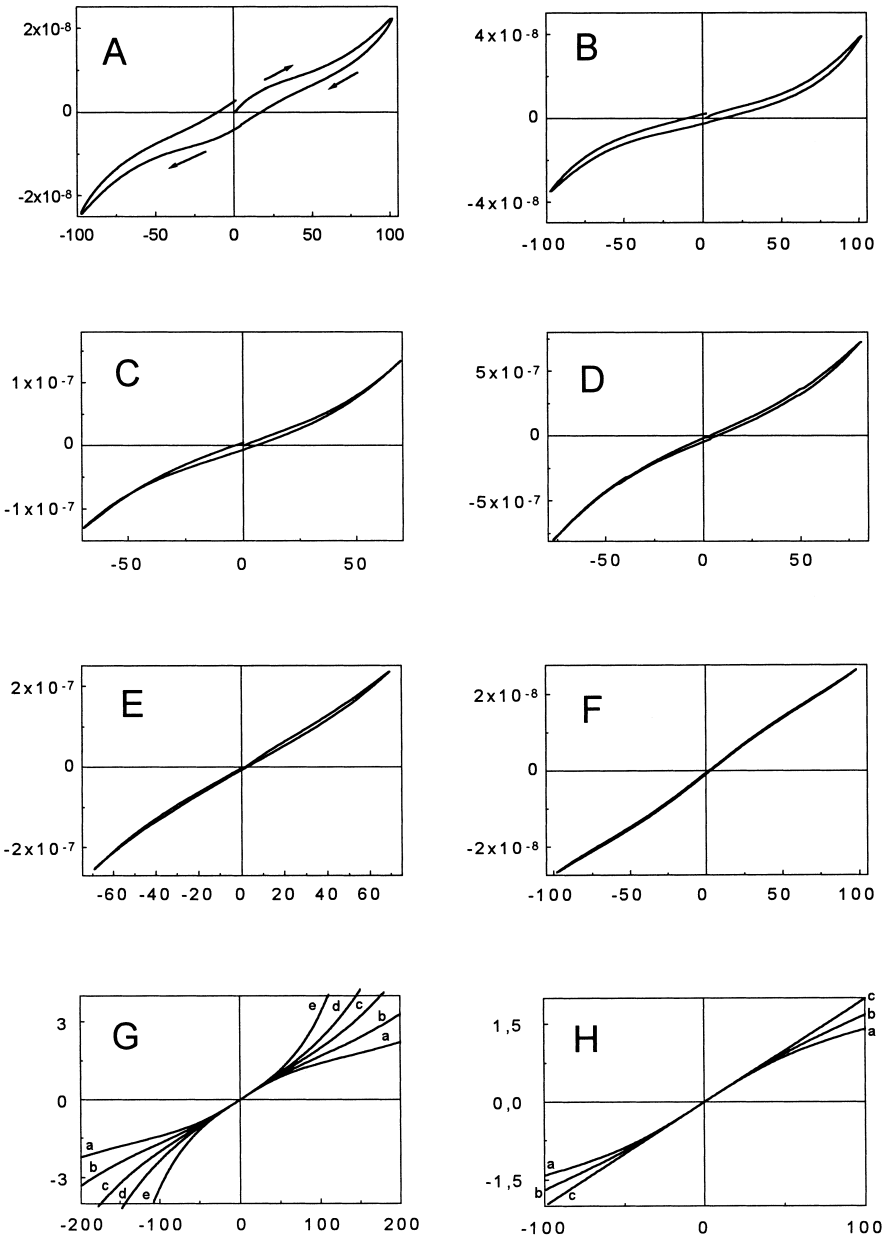

Fig. 8. A–D: Current–voltage curves for various sodium chloride solutions: A = 0.001, B = 0.01, C = 0.1, D = 1 M; scan rate: 2 mV/s. The arrows in A show the mode of curve registration (start at zero potential); $Eu(fod)_3$ concentration: 50 μM; membrane area: 1.5 mm^2; current in ampere, membrane voltage in millivolt. E–H: Experimental and calculated current–voltage curves. E = 0.1 M NaCl (other membranes as in curves A–D). F = 0.1 M $EuCl_3$. $Eu(fod)_3$ concentration: E: 50 μM; F: 20 μM; membrane area: 1.5 mm^2; current in ampere, membrane voltage in millivolt. G = calculated curves according to Eq. 4 with variation of the symmetry factor α. a: $\alpha = 0.1$, b: $\alpha = 0.15$, c: $\alpha = 0.2$, d: $\alpha = 0.25$, e: $\alpha = 0.4$. H: Some curves from G in an extended potential scale. a: $\alpha = 0.1$, b: $\alpha = 0.15$, c: $\alpha = 0.2$. Current axes in G and H represent the quotient j/j^0 according to Eq. 4, membrane potential in millivolt.

ber was varied by the addition of appropriate amounts of NaCl stock solution. We found that the membrane potential changed by about 70 mV by changing the quotient of both concentrations by a factor of 10. Furthermore, we observed that the potential of the chamber with the low NaCl concentration became positive in comparison to that of the chamber of the high concentration. The mentioned

findings show that the membrane potential results from the transfer of sodium ions across the membrane. Carrying out analogous studies with other electrolyte solutions (KCl, CsCl) we found shifts of the membrane potential in the same direction and in the same order of magnitude as described above for NaCl.

For another experiment we used $Eu(dpm)_3$ instead of $Eu(fod)_3$ for modification of the membrane (see Fig. 1 for the chemical composition of the europium complexes). The investigations showed that even for concentrations as large as 200 μM, $Eu(dpm)_3$ does not enhance the membrane conductivity significantly although this complex is also located in the membrane interior as found by NMR experiments.

Then, we carried out experiments with another membrane forming lipid, namely DPhyPC, which has no double bond in the hydrocarbon chain. The experiment answered the question of whether the interactions of $Eu(fod)_3$ near the double bond of DOPC which were proposed by the NMR measurements are responsible for the incorporation of $Eu(fod)_3$ into the membrane. Provided this is true then $Eu(fod)_3$ would not show any influence on the conductivity of the DPhyPC membrane. The experiment definitely showed that the conductivity of $Eu(fod)_3$ modified DPhyPC membrane increases to the same extent as observed for DOPC membranes.

Finally, we carried out experiments with other electrolytes (0.1 M solutions of KCl, LiCl, CsCl, Na_2SO_4 and $EuCl_3$). The current–voltage behavior of the $Eu(fod)_3$-modified membranes in the changed electrolyte is – with the exception of the europium electrolyte – analogous to those described for NaCl. In the case of $EuCl_3$ (Fig. 8F), the curves have a distinctly lower current amplitude than for NaCl as well as another curve shape which is converse to the other curves.

4. Theory

An important result of the NMR investigations was the finding that the $Eu(fod)_3$ molecules penetrate into the hydrocarbon part of the membrane but also interact with the hydrophilic part of the bilayer.

This finding supports the idea that the modifier molecules are able to form an ion conducting structure (defect structure) inside the membrane which facilitates the ion transfer through the membrane.

For the macroscopic description of the membrane ion transfer, two types of models are suitable: kinetic and thermodynamic model ideas. The thermodynamic ideas are based on the Nernst–Planck equation [9]. Integration of the latter differential equation by omitting the inner membrane charge gives the Goldman equation [10]. The application of the Goldman equation to our experiments with equal ion concentrations on both sides of the membrane would give linear current–voltage curves. Indeed, our measurements gave exponentially and other non-linear shaped current–voltage curves (see Fig. 8B–E). This finding suggests kinetic model ideas for the description of the $Eu(fod)_3$-facilitated ion transfer. The basis of these ideas is the assumption of potential-dependent energy barriers for the ion transfer across the membrane (see Fig. 9).

The electrostatic energy barrier which a small ion like the sodium ion has to overcome to be placed inside the membrane is quite high (curve A in Fig. 9). According to Born's equation [11] an energy for the ion transition from the solution into the membrane interior of about 170 kJ/mol results for a monovalent ion of 2 Å radius [12]. Regarding the

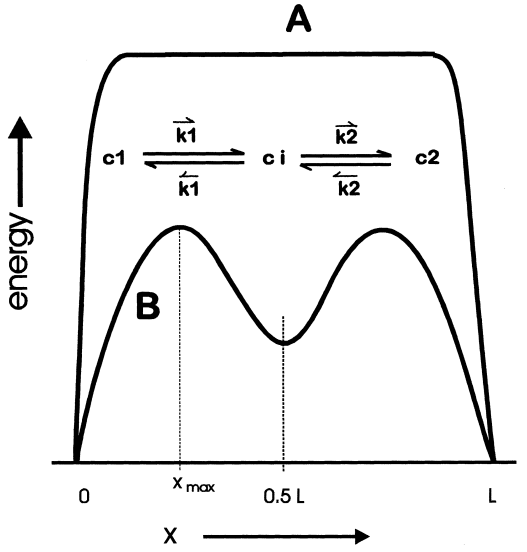

Fig. 9. Hypothetical energy schemes for the membrane ion transfer. Curve A: electrostatic energy barrier of the membrane for small ions; curve B: assumed reduction of the energy barrier by $Eu(fod)_3$. x = distance from the left membrane surface, L = thickness of the membrane interior.

action of the modifier molecules on the energetics of the ion transfer, one may assume that $Eu(fod)_3$ reduces the energy for the ion transfer in both lipid layers to the same extent as depicted in curve B in Fig. 9. The energy barriers for the $Eu(fod)_3$-assisted ion transfer could be the result of either geometrical constraints, e.g. a narrow pass in the assumed defect structure which requires a dehydration of the sodium ion, or specific interactions of the permeating ion along its way through the membrane. It cannot be excluded that the possibility of more than two barriers exists which influence the ion transfer. Nevertheless, the two-barrier model seems to be the simplest model which is kinetically equivalent to the case under consideration. Assuming both barriers are at the same distance from the membrane surfaces, the rate of the membrane ion transfer can be described by the following current–voltage equations:

$$j_1 = zF\left[c_1 \overrightarrow{k}_1 e^{\alpha\phi\varphi} - c_i \overleftarrow{k}_1 e^{-(0.5-\alpha)\phi\varphi}\right],$$

$$j_2 = zF\left[c_i \overrightarrow{k}_2 e^{(0.5-\alpha)\phi\varphi} - c_2 \overleftarrow{k}_2 e^{-\alpha\phi\varphi}\right] \qquad (1a, b)$$

with j_1 and j_2 as the currents through the both membrane monolayers, the (inner) membrane potential φ and $\phi = zF/RT$ (z = ionic charge, F = Faraday constant, R = gas constant and temperature T). The rate constants k_i in Eq. 1a,b are governed by the energy barriers according to barrier ideas which were applied in the past successfully for the description of the kinetics of electron transfer at electrodes [13], for the ion transport in solutions [14] and for the ion permeation through narrow protein channels in biomembranes [15]. The relationship between rate constants and energy barriers will not be further discussed here.

The membrane surface concentrations c_1 and c_2 are assumed to be obtained from the bulk concentrations c_{1b} and c_{2b} according to the following equilibrium relations: $c_1 = K_1 c_{1b}$ and $c_2 = K_2 c_{2b}$ with equilibrium constants K_i which also depend on the amount of modifier inside the membrane. Another important parameter in Eq. 1a,b is the symmetry factor α which governs the location of the energy maximum x_{max} inside the membrane ($\alpha = x_{max}/L$). The symmetry factor has a considerable influence on the course of membrane current–voltage curves as will be shown below.

The substitution of the rate constants k_i by both exchange current densities:

$$j_1^0 = zFc_1^0 \overrightarrow{k}_1 = zFc_i^0 \overleftarrow{k}_1$$

and

$$j_2^0 = zFc_i^0 \overrightarrow{k}_2 = zFc_2^0 \overleftarrow{k}_2$$

with c_1^0 and c_2^0 as the surface concentration in the zero current case yields the current–voltage relationships Eq. 1a,b in a more general form:

$$j_1 = j_1^0\left[\frac{c_1}{c_1^0} e^{\alpha\phi\varphi} - \frac{c_i}{c_i^0} e^{-(0.5-\alpha)\phi\varphi}\right],$$

$$j_2 = j_2^0\left[\frac{c_i}{c_i^0} e^{(0.5-\alpha)\phi\varphi} - \frac{c_2}{c_2^0} e^{-\alpha\phi\varphi}\right] \qquad (2a, b)$$

Eq. 2a,b contains the unknown ion concentration c_i in the energy minimum of scheme Fig. 9B. This concentration can be calculated from the steady-state condition $j_1 = j_2 = j$ by using Eq. 2a,b. Assuming that the concentrations c_1 and c_2 in Eq. 2a,b are independent of the current j and $j_1^0 = j_2^0 = j^0$, the concentration c_i results as:

$$c_i = c_i^0 \cdot \frac{e^{\alpha\phi\varphi} + e^{-\alpha\phi\varphi}}{e^{(0.5-\alpha)\phi\varphi} + e^{-(0.5-\alpha)\phi\varphi}} \qquad (3)$$

Introducing the calculated c_i into Eq. 2a or Eq. 2b gives the following stationary current–voltage relationship of the membrane:

$$j = j^0 \cdot \left[\frac{e^{0.5\phi\varphi} - e^{-0.5\phi\varphi}}{e^{(0.5-\alpha)\phi\varphi} + e^{-(0.5-\alpha)\phi\varphi}}\right] \qquad (4)$$

In the borderline case of either $\alpha = 0$ or $\alpha = 0.5$, the quotient of Eq. 4 leads to the tanh function or the sinh function, respectively.

Eq. 4 is a mathematical function which depends on two parameters, namely j^0 and α. The shape of the current–voltage curves is determined by the symmetry factor α. Fig. 8G shows the influence of this model parameter on the curves. As shown in the figures the calculation gave very differently shaped curves. For $\alpha \geq 0.25$ the curves have an exponential course which is more significant the larger α is. The more interesting curves results for $\alpha < 0.25$. At the beginning the current increases relatively fast but then the slope of the curve decreases. The curves pass a point of inflexion with a pronounced linear

curve shape at both sides. This linear range increases with decreasing α. After passing the inflexion point the current increases exponentially towards higher potentials.

In summarizing the model investigations, it should be pointed out that by using the kinetic model introduced above current–voltage curves with different shapes can be calculated, analogous to those curves observed in the experiments. In all cases the curves have the same course in both potential directions as predicted by Eq. 4. The relationship Eq. 4 can also be used to estimate the exchange current density and the symmetry factor from experimental curves. Table 2 shows the parameters of the model curves which best fit the experimental curves with regard to a minimum of the sum of the squared residuals.

Table 2 illustrates that j^0 increases with increasing NaCl concentration, but not as much as predicted by the model. The symmetry factor also changes with the electrolyte concentration. This means that according to our kinetic model the location of both energy barriers inside the membrane varies depending on the concentration and kind of electrolyte used in the experiments.

The calculation of the membrane impedance requires the alternating current $\tilde{j}$ which results from the voltage perturbation: $\Delta\varphi = \Delta\varphi^0 e^{i\omega t}$. The current $\tilde{j}$ is composed of the transport current j (according to Eq. 4) and the capacitative current j_c:

$$\tilde{j} = j + j_c = j + i\omega C_M \Delta\varphi \quad (5)$$

with the membrane capacitance C_M and the angular velocity $\omega = 2\pi f$ (f = frequency).

Because of the small $\Delta\varphi$ used in impedance spectroscopy, the exponential terms in the transport current j can be linearized. For the zero membrane potential which was the actual dc potential in the impedance experiments, the linearization of Eq. 4 yields $j = 0.5 j^0 \phi \Delta\varphi$ for $\varphi = \Delta\varphi$. By using this current, the impedance Z is obtained according to:

$$Z = \frac{d\varphi}{d\tilde{j}} = \frac{1}{0.5\phi j^0 + i\omega C_M} = \frac{1}{\frac{1}{R_M} + i\omega C_M} \quad (6)$$

Eq. 6 reflects the dependence of the membrane impedance on the different model parameters. The equation also illustrates that Z is equivalent to a parallel circuit of the membrane capacitance and the membrane resistance. The resistance R_M is coupled with the exchange current density j^0 according to $R_M = \Delta\varphi / j = 2/\phi j^0$. This interdependence can be used to calculate j^0 from the low frequency part of the impedance spectrum. It should be mentioned that the impedance in Eq. 6 does not regard the influence of ion diffusion in the layer adjacent to the membrane on the ion transfer. The consideration of diffusion would require a time-dependent calculation of the membrane surface concentrations (c_1 and c_2 in Eq. 1a,b) according to Fick's second law.

Table 2
Model parameters derived from the measured membrane current–voltage curves

Experiment	Solution	j^0 (A cm^{-2})	α
Fig. 7B	0.01 M NaCl	7×10^{-7}	0.42
Fig. 7C	0.1 M NaCl	5×10^{-6}	0.38
Fig. 7D	1 M NaCl	2.3×10^{-5}	0.28
Fig. 7E	0.1 M NaCl	1.1×10^{-5}	0.24
Fig. 7F	0.1 M $EuCl_3$	1×10^{-6}	0.15

α = symmetry factor, j^0 = exchange current density, according to Eq. 4.

5. Discussion

Preliminary studies had shown that the fluorinated europium complex $Eu(fod)_3$ enhances the electric conductivity of planar lipid membranes. This surprising observation caused us to start different experiments for investigating the mentioned membrane effect.

UV-Vis experiments concerning the partition of $Eu(fod)_3$ between octanol and water showed that the complex is preferably located in the hydrophobic liquid. An analogous partition behavior was observed in aqueous solutions of DOPC liposomes. We found that most of the modifier molecules were resorbed by the liposomes.

^{1}H NMR measurements on the liposomes should answer the question of the localization of the modifier at the membrane. The measurements revealed that the europium complex induces a shift of the proton NMR signals at different parts of the membrane lipid.

Although the NMR measurements provided some information about the location of the modifier at the

membrane we have no information about the detailed arrangement of the $Eu(fod)_3$ molecule(s) in the lipid matrix and about the resulting defect structure inside the lipid matrix which enables the ions to pass the membrane. The ester group of the lipid may be considered one binding site for the complex. However, the opposite direction and the magnitudes of the shifts for the hydrophobic and the hydrophilic proton groups demonstrate two different orientations of the probe in the liposome. The angle between the principal symmetry axis of the complex and the vector metal/proton is smaller than 54° for the groups near the olefinic bond but greater than 54° for the choline head protons. Additionally, the observed diametrically opposed changes of the NMR data (Figs. 4 and 5) for the head group signal and the signals of the olefinic region going from $Eu(fod)_3$ to the more hydrophobic $Eu(dpm)_3$ refer to the existence of two independent binding sites. Using the above NMR data the partition of the lanthanide complexes within the SUV can be schematically presented as in Fig. 10.

The formation of ion conducting membrane defects is dependent on the structure of the europium complex. Using the europium complex $Eu(dpm)_3$ – without any fluorine groups – no enhancement of the membrane conductivity occurs, although this modifier also penetrates into liposomes, as NMR measurements revealed. In agreement with our partition study in micelles it can be concluded that the introduction of CF_2 and CF_3 groups reduces the lipophilicity and favors the partition within the hydrophilic part of the membrane.

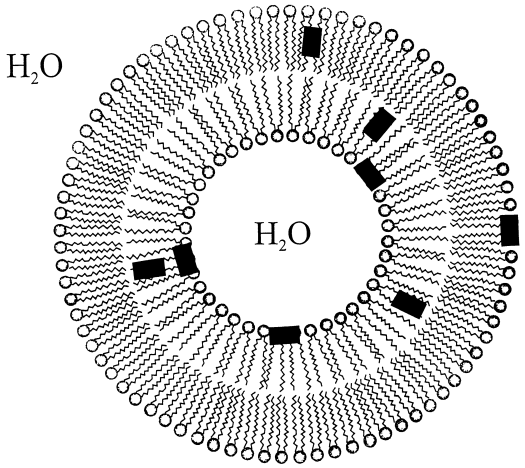

Fig. 10. Model of the partition of the lanthanide complex within the liposome. For demonstration of the two different orientations of the principal magnetic axis in relation to the lipid layer the octahedral structure of the complex was not considered.

The preferential accumulation of the hydrophobic paramagnetic complex in the inner lipid layer may be caused by the geometric packing constraints in small vesicles. The cone-like arrangement of lipid molecules favors an enrichment between the fatty acid chains of the inner lipid layer. However, the unexpected enrichment of the probes at the internal choline head group could reflect deviations in the structure of the enclosed small water droplet in comparison to the outer hydration shell of the liposome.

The increase in the conductivity does not occur if the $Eu(fod)_3$ molecule is added to only one side of the membrane. This finding is a hint that the formation of an ion conducting path through the membrane requires the presence of the modifier in both lipid layers. The modifier molecules could act as a kind of wedge which loosens the lipid matrix providing a path for the ion transfer through the membrane. The observation that only $Eu(fod)_3$ is able to transport cations could be explained with the thesis that the fluorine groups of $Eu(fod)_3$ mediate the transition of cations from the surface into the lipid layer. This thesis would explain the observation that $Eu(dpm)_3$, without any fluorine groups, is unable to enhance the ion permeation through the membrane.

Impedance measurements showed that the membrane conductivity increases approximately with the $Eu(fod)_3$ concentration. This finding can be understood by an appropriate increase of the $Eu(fod)_3$-induced defect structures inside the membrane. Increasing the ion concentration increases the electric conductivity of the modified membrane not to the same extent as the electrolyte concentration increases. This refers to a limitation of the ion transport which could be due to a limitation of the permeation rate of ions along the assumed defect structures inside the membrane.

Another reason could be a deviation from the assumed equilibrium partition of the ions between the solution and the surface compartment of the membrane according to the model ideas discussed in Section 4.

However, measurements of the current–voltage behavior of $Eu(fod)_3$-modified membranes in depen-

dence on the ion concentration gave differently shaped curves. We found not only exponential current–voltage curves but also curves with a more complicated shape.

This finding and the observation that both lipid layers have to be modified for the realization of the ion permeation suggest a kinetic model with two energy barriers for the ion transfer inside the membrane. The current–voltage curves derived by the use of this model enable the calculation of the different types of current–voltage curves observed at Eu $(fod)_3$-modified membranes. For the interpretation of the curves it has to be assumed that the location of both energy barriers of the kinetic model can vary with the concentration and the kind of the electrolyte. This variation might be due to changes in the structure of the assumed membrane defects for the ion transfer.

By comparing the experimental current curves with calculated model curves, we estimated the two model parameters: the exchange current density j^0 and the symmetry factor α which describes the barrier location inside the membrane. The kinetic parameter j^0 is coupled with the rate constant for the ion transfer across the membrane. Indeed, the rate constant cannot be separated because of the unknown equilibrium constant for the ion distribution on the membrane surfaces.

Acknowledgements

We are grateful to the referees for their useful comments which helped in improving the quality of this article.

References

[1] S. Braun, H.O. Kalionowski, S. Berger, 150 and More basic NMR-experiments, 2nd edn., Wiley-VCH, New York, 1998.
[2] J.-C. Bunzli, Lanthanide Probes in Life, Chemical and Earth Sciences, Elsevier, Amsterdam, 1989.
[3] E.F.G. Dickson, A. Pollak, E.P. Diamandis, J. Photochem. Photobiol. B Biol. 27 (1995) 3–19.
[4] H. Sprinz, K.D. Schulze, Z. Phys. Chem. 205 (1998) 99–111.
[5] K.D. Schulze, J. Dittmar, H. Sprinz, Z. Phys. Chem. 205 (1998) 83–97.
[6] K.D. Schulze, J. Chem. Phys. 238 (1998) 495–505.
[7] H. Sprinz, E. Winkler, H. Schäfer, Isotopenpraxis 17 (1981) 171–173.
[8] J.H. Fendlar, E.J. Fendlar, Catalysis in Micellar and Macromolecular Systems, Academic Press, New York, 1975.
[9] G. Adam, P. Läuger, G. Stark, Physikalische Chemie und Biophysik, Springer, Berlin, 1995.
[10] D.E. Goldman, J. Gen. Physiol. 27 (1943) 37–60.
[11] M. Born, Z. Phys. 1 (1920) 45–48.
[12] R.B. Gennis, Biomembranes – Molecular Structure and Function, Springer, New York, 1990.
[13] T. Erdey-Gruz, M. Volmer, Z. Phys. Chem. 150A (1930) 203–213.
[14] B.I. Zwolinski, H. Eyring, C.E. Reese, J. Phys. Colloid Chem. 53 (1949) 1426–1453.
[15] P. Läuger, Biochim. Biophys. Acta 311 (1973) 423–441.